Mid- and High-Power Passively *Q*-Switched Microchip Lasers

John J. Zayhowski, Colby Dill III, Chris Cook, and John L. Daneu
MIT Lincoln Laboratory, Lexington, MA 02420-9108

Abstract: Passively *Q*-switched Nd:YAG microchip lasers have been developed that produce up to 250 μJ/pulse at 1.064 μm, with a pulse duration of 380 ps. The infrared output has been harmonically converted to 532, 355, and 266 nm with high efficiency.
OCIS codes: (140.3480) Lasers, diode-pumped; (140.3540) Lasers, *Q*-switched; (140.3580) Lasers, solid-state; (190.0190) Nonlinear optics

Introduction

Passively *Q*-switched microchip lasers are simple, compact, robust sources of short-pulse laser radiation with high peak power and nearly ideal mode quality. Although there are some reports on high-power devices (pumped with 10–12 W of diode power) [1–4], most of the work on passively *Q*-switched microchip lasers has concentrated on lasers pumped with ~1 W of diode power [3–12]. Here, we give a detailed description of several mid- and high-power lasers in a series of devices recently developed at Lincoln Laboratory. These passively *Q*-switched microchip lasers were designed to be pumped with the output of 3- and 10-W high-power fiber-coupled 808-nm diode-laser arrays. The most powerful of these lasers produces 250 μJ/pulse at 1.064 μm, with a pulse duration of 380 ps and peak power in excess of 560 kW. The infrared output of these devices has been harmonically converted to 532, 355, and 266 nm with high efficiency.

The devices reported here were built and tested for several different applications. There was no attempt to ensure that test conditions on different devices were equivalent, or that the same tests were performed on each device. For example, the pulse energies and thresholds of the lasers are dependent on the magnification of an intermediate lens. Optimization for high energy at low repetition rates requires different focusing than optimization for high repetition rates. Some applications required high-repetition-rate operation, others did not. Each of the lasers was optimized for a particular application under different operating conditions. None-the-less, the results reported here give a good idea of the capabilities of the technology discussed.

Mid-Power Passively *Q*-Switched Microchip Lasers

The 3-W-pumped mid-power microchip lasers discussed here (MPMCL-1, MPMCL-2, and MPMCL-3) all comprise a piece of Nd:YAG diffusion bonded to a 3-mm-long piece of Cr^{4+}:YAG. For MPMCL-1 and MPMCL-2, the Nd:YAG is 3 mm long. For MPMCL-3, the Nd:YAG has a length of 9 mm. The Nd:YAG in all of the devices is doped at 1.1 wt.% Nd; the Cr^{4+}:YAG has an unsaturated absorption of 1.5 cm^{-1} at 1.064 μm. In addition to these two materials, devices MPMCL-2 and MPMCL-3 have a piece of undoped YAG diffusion bonded to the Cr^{4+}:YAG on the face opposite the Nd:YAG, as shown in Fig. 1. The dimensions of the crystals are given in Table 1. Dielectric coatings are applied directly on the crystals. The input coating, deposited on the Nd:YAG, is antireflecting at the pump wavelength (808 nm) and highly reflecting (>99.9%) at the oscillating frequency. The output coating on all of the mid-power devices has a reflectivity of 60% at the oscillating frequency (1.064 μm).

OSA TOPS Vol. 26 Advanced Solid-State Lasers
Martin M. Fejer, Hagop Injeyan, and Ursula Keller (eds.)

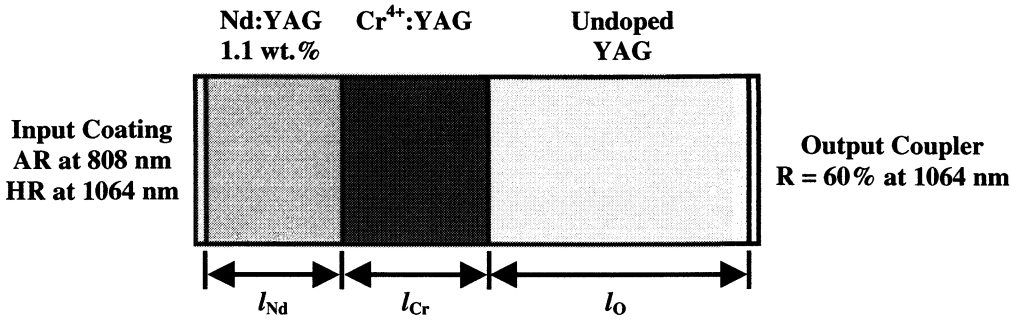

Fig. 1. Schematic of 3-W-pumped mid-power passively Q-switched microchip lasers.

The undoped YAG in MPMCL-2 and MPMCL-3 is used to lengthen the cavity in a way that maintains the robustness of the device. The increased cavity length results in a larger oscillating-mode diameter and, therefore, more efficient use of the pump. In addition, it leads to a longer pulse length, which can be advantageous for pumping optical parametric oscillators [1]. The Cr^{4+}:YAG is kept near the center of the cavity so that spatial hole burning in the saturable absorber has the largest possible effect on maintaining single-longitudinal-mode operation of the laser. The faces of the composite Nd:YAG/Cr^{4+}:YAG/undoped-YAG material system are polished flat, to a parallelism of better than 10 μrad.

The microchip lasers are cut to a nominal 2 × 2-mm cross section and bonded to a gold-coated oxygen-free-copper heatsink with thermally conductive epoxy. Before bonding, the bonded sides of the lasers are ground flat for good thermal contact. The surfaces to be bonded are meticulously cleaned to ensure the minimum bond thickness and avoid the formation of bubbles in the epoxy. Typical epoxy thicknesses are 5 μm.

To pump the mid-power microchip lasers, the 3-W output of a fiber-coupled diode-laser array is passed through a protective window and imaged into the gain medium (Nd:YAG) with an antireflection-coated, matched pair of aspheric lenses (f = 11 mm, NA = 0.25). The positions of the fiber end, lens pair, and microchip laser are empirically optimized, but typically result in a unity magnification of the fiber facet (core diameter = 100 μm, NA = 0.2) in the Nd:YAG. The protective window is coated to be antireflecting at the pump wavelength and highly reflective at both the lasing wavelength and its second harmonic. This prevents any high-peak-power laser radiation (and its second harmonic) from being coupled into the fiber, propagating back to the pump diodes, and causing damage. The protective window is also used to hermetically seal the microchip laser head.

The repetition rate of the passively Q-switched lasers is controlled by pulsing the pump diodes. The length of the diode ON pulse is set to allow exactly one output pulse from the microchip laser for each pulse of the diodes. MPMCL-1 and MPMCL-2 can be pulse pumped with 3 W of optical power.

Table 1. 3-W-Pumped Mid-Power Passively Q-Switched Microchip Laser Parameters

Device	Nd:YAG	Cr^{4+}:YAG	Output YAG Cap	Cr^{4+}:YAG Absorption	Output Coupler
	l_{Nd} (mm)	l_{Cr} (mm)	l_O (mm)	α (cm^{-1})	R (%)
MPMCL-1	**3**	**3**	**0**	**1.5**	**60**
MPMCL-2	**3**	**3**	**6**	**1.5**	**60**
MPMCL-3	**9**	**3**	**12**	**1.5**	**60**

Table 2. Mid-Power Device Characteristics at 500 Hz

Device	Pump Power (W)	Pulse Energy (μJ)	Pulse Width (ps)	Beam Waist (μm)	Peak Power (kW)	Peak Intensity (GW/cm^2)	Peak Fluence (J/cm^2)
MPMCL-1	**3**	**30**	**700**	**60**	**37**	**0.65**	**0.53**
MPMCL-2	**3**	**40**	**1200**	**70**	**29**	**0.37**	**0.52**
MPMCL-3	**5**	**65**	**2200**	**85**	**25**	**0.22**	**0.57**
MPMCL-1	**10**	**100**	**650**	**85**	**132**	**1.16**	**0.88**
MPMCL-2	**10**	**150**	**1000**	**100**	**129**	**0.82**	**0.95**
MPMCL-3	**10**	**180**	**2000**	**120**	**77**	**0.34**	**0.80**

At low pulse repetition rates, MPMCL-1 produces 30 μJ/pulse with a 700-ps pulse duration. MPMCL-2 produces 40 μJ/pulse with a 1200-ps pulse duration. MPMCL-1 can also be cw pumped, to produce 330 mW of infrared output at 16-kHz repetition rate. MPMCL-2 cannot be cw pumped. With 3 W of pump power, it has a maximum pulse repetition rate of ~3 kHz. MPMCL-3 requires more than 3 W to reach threshold. With 5 W of pump power it can be pulsed at up to 2.5 kHz and produces 65-μJ pulses of 2200-ps duration. The performance of the mid-power passively *Q*-switched microchip lasers is summarized in Table 2 for a pulse repetition rate 500 Hz.

With the use of 3 (or 5) W of pump power, all of the mid-power devices operate in a linearly polarized, single longitudinal mode, with diffraction-limited output. When pulse pumped, the amplitudes and pulse widths are stable to within 1%. When MPMCL-1 is cw pumped, its output bifurcates at pulse repetition rates above 15 kHz. Alternating pulses are in different longitudinal and polarization modes, each with slightly different amplitude.

The mid-power microchip lasers can also be pumped with 10 W of diode power, producing ~3 times more energy per pulse than when pumped with 3 W. Similar devices, pumped with 12 W, have been previously reported [1–3]. The performance with 10-W pumping at a pulse repetition rate of 500 Hz is included in Table 2. When pumped with 10 W, none of the mid-power devices maintains single-mode performance at pulse repetition rates much above 2 kHz. Multimode oscillation is often followed by damage to the output facet of the laser.

High-Power Passively *Q*-Switched Microchip Lasers

The four 10-W-pumped high-power infrared microchip lasers discussed here (HPMCL-1, HPMCL-2, HPMCL-3, and HPMCL-4) comprise a four-crystal sandwich of undoped YAG, Nd:YAG, Cr^{4+}:YAG, and undoped YAG, diffusion bonded to each other in that order, as shown in Fig. 2. The Nd:YAG in all of the devices is doped at 1.1 wt.% Nd. HPMCL-2 uses a piece of Cr^{4+}:YAG with an unsaturated absorption of 1.5 cm^{-1} at 1.064 μm. For the rest of the devices, the unsaturated absorption of the Cr^{4+}:YAG is 6 cm^{-1} at 1.064 μm. The dimensions of the crystals are given in Table 3. Devices HPMCL-1 and HPMCL-2 have an unsaturated round-trip loss due to the saturable absorber of 83%. The unsaturated round-trip loss in HPMCL-3 and HPMCL-4 is 93%. Dielectric coatings are applied to the undoped YAG endcaps. For all devices, the input-side coating is antireflecting at the pump wavelength and highly reflecting (>99.9%) at the oscillating frequency. The output coatings of HPMCL-1 and HPMCL-2 have a reflectivity of 40% at 1.064 μm. The reflectivity of the output coatings of HPMCL-3 and HPMCL-4 is 26%.

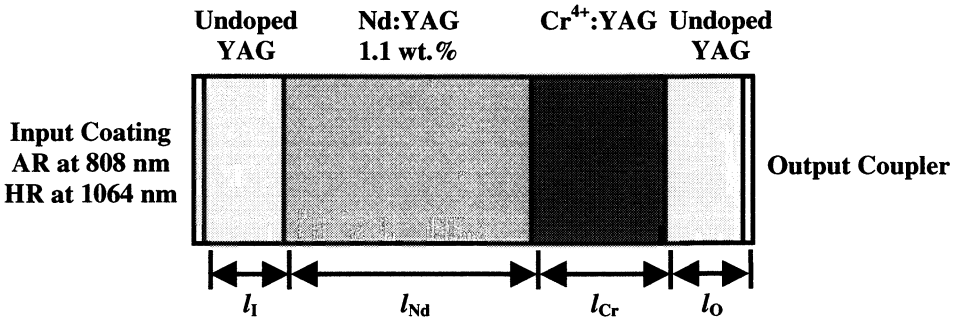

Fig. 2. Schematic of 10-W-pumped high-power passively *Q*-switched microchip lasers.

In the high-power lasers, the undoped YAG endcaps are used primarily to improve the damage threshold of the devices. The use of undoped endcaps has become common practice in high-power lasers. Since there is no absorption of pump or laser radiation in the undoped materials, thermal stress at the YAG/dielectric-coating and dielectric-coating/air interfaces is reduced. This improves the damage threshold of the coatings. It has also been observed that, independent of thermal stress, undoped materials have a higher damage threshold than doped materials, and the damage usually occurs at the surface of the materials. Diffusion bonding buries the Nd:YAG and Cr^{4+}:YAG ends, protecting them from damage.

The faces of the composite undoped-YAG/Nd:YAG/Cr^{4+}:YAG/undoped-YAG material system are polished to a parallelism of better than 10 μrad. The surfaces are polished so that there are no apparent scratches, sleeks, or digs in the active region when viewed with a Nomarski microscope at magnifications up to 800×. This level of surface finish is used to avoid the high fields that can arise at surface irregularities and nucleate damage. (The intensity of the infrared beam exiting the laser is as high as 10 GW/cm^2; we were concerned about field-induced damage.) The surfaces are meticulously cleaned before applying high-damage-threshold dielectric coatings. The coatings are fabricated using a high-temperature ion-assisted deposition process. The output coatings are finished with a half-wave (at 1.064 μm) layer of SiO_2 to further increase the damage threshold and robustness of the devices. Having taken the precautions described in this paragraph, we have not observed coating damage to any of the high-power devices over a cumulative operating time of several hundred hours.

The high-power microchip lasers are cut to a nominal 2 × 2-mm cross section and bonded to a gold-coated oxygen-free-copper heatsink with thermally conductive epoxy, in the same way as the mid-power lasers. For high-repetition-rate operation of the 10-W-pumped devices, it is necessary to heatsink the lasers from the top as well as the bottom. A U-shaped piece of oxygen-free copper is carefully machined to contact the top of the laser and the bottom heatsink on both sides of the laser, within a

Table 3. 10-W-Pumped High-Power Passively *Q*-Switched Microchip Laser Parameters

Device	Input YAG Cap l_I (mm)	Nd:YAG l_{Nd} (mm)	Cr^{4+}:YAG l_{Cr} (mm)	Output YAG Cap l_O (mm)	Cr^{4+}:YAG Absorption α (cm^{-1})	Output Coupler R (%)
HPMCL-1	**1**	**3**	**1.5**	**1**	**6**	**40**
HPMCL-2	**1**	**4**	**6**	**1**	**1.5**	**40**
HPMCL-3	**1**	**3**	**2.25**	**1**	**6**	**26**
HPMCL-4	**1**	**4**	**2.25**	**3**	**6**	**26**

Table 4. High-Power Device Characteristics at 500 Hz

Device	Pump Power (W)	Pulse Energy (μJ)	Pulse Width (ps)	Beam Waist (μm)	Peak Power (kW)	Peak Intensity (GW/cm^2)	Peak Fluence (J/cm^2)
HPMCL-1	**3**	**70**	**400**	**55**	**150**	**3.2**	**1.5**
HPMCL-1	**10**	**130**	**390**	**70**	**286**	**3.7**	**1.7**
HPMCL-2	**10**	**225**	**700**	**90**	**276**	**2.2**	**1.8**
HPMCL-3	**11**	**200**	**310**	**60**	**554**	**9.8**	**3.5**
HPMCL-4	**15**	**250**	**380**	**60**	**565**	**10.0**	**4.4**

tolerance of 5 μm. The length of the heatsink is equal to the length of the laser. Thermal epoxy is applied to the three contact areas, the top heatsink is clamped in place, and the epoxy is cured. Contact to the sides of the laser is avoided. Thermal contact to both the top and bottom of the laser results in symmetry in the thermal loading of the device and prevents thermal destabilization of the microchip cavity. We have noticed, however, that at high duty cycles the polarization axis of the laser can switch from being defined by internal properties of the YAG crystals to being oriented with the thermal stress induced by the heatsink geometry. This problem can be avoided by pretesting and properly aligning the microchip lasers before they are diced into 2 × 2-mm devices.

To pump the high-power microchip lasers, the 10-W output of a fiber-coupled diode-laser array is passed through a protective window and imaged into the gain medium (Nd:YAG) with an antireflection-coated, matched pair of aspheric lenses. The positions of the fiber end, lens, and microchip laser are empirically optimized, but typically result in a ~0.5 magnification of the fiber facet (core diameter = 250 μm, NA = 0.2) in the Nd:YAG. All of the elements of the high-power microchip laser heads, with the exception of the laser itself and the top heatsink described above, are the same as for the mid-power devices.

For HPMCL-1 to reach threshold with a 10-W pump requires a diode ON pulse of only 140 μs, a duration well below the spontaneous lifetime of the upper laser level. This device can be pumped with as little as 6.5 W from the 10-W diode-laser array and produces 130-μJ pulses with 390-ps pulse width at low repetition rates. A high-brightness 3-W diode-laser array has also been used to pump HPMCL-1. When pumped with 3 W, the beam cross section and the output power of the laser are reduced by about a factor of 2. HPMCL-2 requires a 300-μs ON pulse with 10-W pumping and produces 225-μJ pulses with 700-ps duration. HPMCL-3 and HPMCL-4 require, respectively, pump powers of 11 and 15 W to reach threshold. They produce 200 μJ in a 310-ps pulse, and 250 μJ in a 380-ps pulse, respectively. The performance of the high-power passively *Q*-switched microchip lasers, at 500-Hz pulse repetition rate, is summarized in Table 4.

Although Table 4 only contains data for a pulse repetition rate of 500 Hz, HPMCL-1 can be pulsed at frequencies up to 5.5 kHz (with 10-W pumping). At high pulse repetition rates the radius of the beam waist decreases to ~60 μm owing to increased thermal mode guiding. The pulse energy decreases to 110 μJ/pulse and the pulse width remains about the same. HPMCL-1 can also be cw pumped to generate ~650 mW of 1.064-μm output. HPMCL-2 operates at repetition rates up to 2 kHz. The beam waist at 2 kHz decreases to 60 μm, without a significant change in its output energy or pulse width. HPMCL-2 cannot be cw pumped. The properties of HPMCL-3 and HPMCL-4 do not change significantly at pulse repetition rates up to 1 kHz; they have not been characterized at higher pulse repetition rates. They cannot be cw pumped.

All of the high-power devices operate in a linearly polarized, single longitudinal mode, with diffraction-limited output. When pulse pumped, the amplitudes and pulse widths are stable to within 1%. When HPMCL-1 is cw pumped, its output bifurcates. Alternating pulses are in different longitudinal and polarization modes, each with slightly different amplitude.

As shown in Table 4, the peak powers of the high-power microchip lasers are several hundred kW, and the peak intensities are several GW/cm^2. Peak fluences are several J/cm^2. These intensities and fluences are the reason for the care that is taken in the surface preparation and coating of the laser facets.

Frequency Conversion

The output of several of the microchip lasers described above has been harmonically converted into the visible and UV. To frequency double the infrared output of the microchip lasers we use low-temperature hydrothermally grown KTP, oriented for Type-II phase matching. The KTP crystals are cut with an orientation of $\theta = 90°$ and $\phi = 27°$. Proper phase matching is achieved for $\theta = 90°$ and $\phi = 24.3°$. Phase matching therefore occurs when the crystal faces are tilted ~4.5° (27° – 24.3° multiplied by an index of 1.7 for KTP) with respect to the infrared output of the microchip laser. This "misorientation" ensures that the KTP does not reflect light directly back into the laser and that multiply reflected beams inside the KTP do not overlap to generate an interference pattern in its output. The input face of the KTP is coated to be antireflecting at 1.064 μm and highly reflecting at 532 nm. The high reflector at 532 nm is used to help protect the pump diodes from any backreflected green light that might otherwise couple into the pump fiber and damage the pump diodes. The output of the KTP is antireflecting at both 1.064 μm and 532 nm.

The damage threshold for KTP is ~1 GW/cm^2. This is above the output intensity of the mid-power microchip lasers. For the mid-power devices, the KTP is positioned next to the output facet of the laser. The peak output intensity of the high-power microchip lasers, however, is much greater than the damage threshold of KTP. For this reason, we mount the KTP so that its input facet is >1.5 cm from the output facet of the microchip laser, where diffraction reduces the peak intensities to below the threshold for bulk material damage in the KTP. Gray tracking (laser-induced photo-refractive damage) can still be a problem. We observe gray tracking in flux-grown materials and high-temperature hydrothermally grown materials at much lower intensities. We have not seen gray tracking in low-temperature hydrothermal KTP, even at 1 GW/cm^2.

The KTP crystals we use are ~5 mm long with a 2 × 2-mm cross section. They are mounted in a V-shaped groove machined in 1/4-in. stainless-steel ball bearings. The V groove is cut so that the center of the KTP sits at the center of the ball bearing. The bottom of the ball bearing (directly opposite the V groove) is drilled and tapped so that an alignment stick can be screwed into it. The ball bearing is mounted in a socket in the microchip-laser mounting block (heatsink) so that the center of the KTP is positioned in the output beam of the microchip laser. For each socket in the mounting block, a V slot is cut from the bottom of the mounting block with its apex at the center of the socket hole. In the plane perpendicular to the microchip-laser output, the slot opens a >90° wedge. In the orthogonal direction the slot is 5/32-in. wide.

To mount the KTP on the laser mounting block, the KTP is epoxied into the ball bearing. The alignment stick is screwed into the ball bearing and lowered through the socket in the mounting block. A spring is used to hold the ball bearing tightly in the socket as the end of the alignment stick is moved with micrometers to properly phase match the nonlinear interaction. The V groove allows the KTP to be rotated by up to 90° to obtain the proper orientation with respect to the polarization of the microchip

Table 5. Average Power Generated by MPMCL-1 and HPMCL-1 at Fundamental and Harmonics

Device	Maximum Pump Power (W)	Pulse Repetition Rate (kHz)	1064-nm Average Power (mW)	532-nm Average Power (mW)	355-nm Average Power (mW)	266-nm Average Power (mW)
MPMCL-1	**3**	**15**	**309**	**186**	**Not tested**	**37**
HPMCL-1	**10**	**5.5**	**605**	**335**	**104**	**66**

laser. (If more than 90° rotation is needed, the nonlinear crystal can be rotated in the ball bearing by 90° increments.) The 5/32-in. slot thickness is sufficient to allow proper alignment in that direction, and the alignment stick can be rotated to obtain proper orientation in the final direction. Alignment is performed actively, with the laser running. When proper alignment is obtained, the top of the ball bearing is epoxied to the mounting block. After the epoxy is cured, the alignment stick is removed.

Typical doubling efficiencies for MPMCL-1 and HPMCL-1, when the KTP is mounted as described above and aligned for maximum doubling efficiency, are about 60%. The performance of these devices, at high pulse repetition rates, is summarized in Table 5. Similar efficiencies are obtained for the other devices. The high-intensity output of these lasers is sufficient to effectively saturate the doubling process in KTP.

Third-harmonic, 355-nm UV output is obtained by summing the 1.064-μm fundamental with the second harmonic of the microchip-laser output in properly oriented BBO using Type-I phase matching. The crystals are ~5 mm long with a 2 × 2-mm cross section. The input face of the BBO is coated to be antireflecting at both input frequencies. The output face is antireflection coated at 355 nm.

When the KTP used for second-harmonic generation is aligned for maximum second-harmonic efficiency, the 1.064-μm radiation at the most intense positions within the laser pulse (both temporally and spatially) is depleted, resulting in poor third-harmonic generation. To more nearly optimize the third-harmonic generation, we rotate the KTP in the plane normal to the incident infrared beam until the second-harmonic efficiency is reduced to ~67% of its maximum value. This ensures that there are about as many usable infrared photons as green photons exiting the KTP. Furthermore, by rotating the KTP in the proper direction, these infrared photons are mostly polarized parallel to the green photons, so that they can be efficiently used in Type-I UV generation [6]. Once the KTP is aligned as described, we mount the BBO in a socket in the mounting block immediately following the one used for the KTP (center-to-center spacing of the sockets is 1/4 in.) and actively align it in a manner similar to that described for the KTP.

Using the procedure described above, we obtain 19 μJ/pulse of 355-nm output at pulse repetition rates up to 5.5 kHz from a nonlinear system built around HPMCL-1. In the near field, the output beam has a nearly diffraction-limited "top-hat" profile in the direction of walk-off in the BBO, with a diameter of ~400 μm. In the opposite dimension the UV beam has a nearly diffraction-limited Gaussian profile, with an effective beam waist (the effective beam waist occurs at the output facet of the microchip laser) of ~50-μm radius.

To obtain fourth-harmonic, 266-nm UV output, we frequency double the 532-nm second harmonic of the microchip laser in properly oriented BBO using Type-I phase matching. The crystals are ~5 mm long with a 2 × 2-mm cross section. The input face of the BBO is coated to be antireflecting at 532 nm; the output face is antireflection coated at 266 nm.

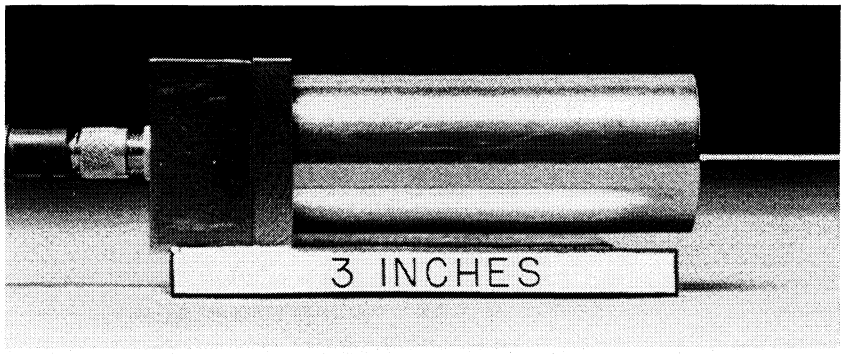

Fig. 3. High-power UV passively *Q*-switched microchip laser head.

In the case of fourth-harmonic generation, the KTP used for second-harmonic generation is aligned for maximum second-harmonic efficiency. The BBO is mounted in the next socket, and aligned as previously described. We obtain 12 μJ/pulse of 266-nm output from a nonlinear system built around HPMCL-1, operating at pulse repetition rates up to 5.5 kHz. A nonlinear system built around MPMCL-1 generates 2.5 μJ/pulse at pulse repetition rates up to 15 kHz. The UV performance of these devices is summarized in Table 5. In the near field, the output beam from both devices has a nearly diffraction-limited top-hat profile in the direction of walk-off in the BBO, with a diameter of ~500 μm. In the opposite dimension the UV beam has a nearly diffraction-limited Gaussian profile, with an effective beam waist of ~50-μm radius.

KTP is a nearly ideal crystal to use for frequency doubling of the microchip-laser output. Very efficient conversion efficiency is obtained at intensities well below the damage threshold. Whether or not KTP is the best crystal to use for frequency doubling as an intermediate step in obtaining the UV harmonics of the high-power passively *Q*-switched microchip laser is questionable, at least if we insist on using no lenses in the system. Since the UV nonlinear crystal, BBO, must follow the KTP crystal, the optical intensity in the BBO is limited to the intensity in the KTP, even though the damage threshold is an order of magnitude higher for the BBO (10 GW/cm^2 for BBO vs 1 GW/cm^2 for KTP). If we were able to increase the optical intensity in the BBO, we would obtain higher efficiencies in the final step of UV generation. For example, by focusing the output of the KTP into a piece of BBO we have obtained 50% conversion of the input 532-nm radiation to 266 nm. In contrast, the efficiency obtained in the systems described above is ~20%. Given the high output intensities of the high-power microchip lasers, the use of other nonlinear crystals for frequency doubling the 1.064-μm output, such as LBO, may result in higher overall UV efficiency. The lower nonlinear coefficient can be offset by the higher intensities available by putting the crystal closer to the output facet of the laser. (The damage threshold for LBO is 18 GW/cm^2, and gray tracking is not an issue.)

In all of our UV devices, we use only zero-outgas epoxies. It has been our experience that the outgassing from epoxies can be cured by the UV laser radiation, and preferentially deposits on the output window of the laser head in the position that the UV radiation passes through the window, destroying the UV beam quality. After all of the nonlinear crystals are mounted, we hermetically seal the laser head in a dry argon environment. A complete, operating high-power UV laser head is shown in Fig. 3.

Summary

We are continuing to push the performance limits of the passively *Q*-switched microchip lasers. The performance characteristics and reliability of the devices discussed here already make them interesting for a variety of applications. In addition to harmonic conversion, the mid- and high-power microchip lasers can be used to pump parametric devices [1–4]. A combination of harmonic and parametric conversion should make it possible to obtain any output wavelength between 5 μm and 200 nm in extremely compact, robust packages. The short pulses are useful for high-precision ranging and imaging. HPMCL-4 is sufficiently powerful to do earth-to-satellite ranging with centimeter accuracy [13]. The high peak powers enable applications in marking, micromachining, laser-induced breakdown spectroscopy (LIBS), matrix-assisted laser desorption and ionization (MALDI), and microsurgery. The focused output of the high-power devices can break down air, with potential applications in the monitoring of effluents and closed-loop process control. The UV output is useful for fluorescence spectroscopy, ionization spectroscopy, and stereolithography for rapid prototyping. Additional applications will continue to surface as this technology becomes more readily available.

Acknowledgements

This work was jointly sponsored by the Department of the Air Force and the NASA Goddard Space Flight Center under Air Force Contract #F19628-95C-0002.

References

1. J. J. Zayhowski, "Microchip optical parametric oscillators," *IEEE Photon. Technol. Lett.* **9**, 925 (1997).
2. J. J. Zayhowski, "Periodically poled lithium niobate optical parametric amplifiers pumped by high-power passively *Q*-switched microchip lasers," *Opt. Lett.* **22**, 169 (1997).
3. J. J. Zayhowski, "Microchip lasers," *Opt. Mat.* **11**, 255 (1999).
4. J. J. Zayhowski, "Passively *Q*-switched microchip lasers and applications," *Rev. Laser Eng.* **26**, 841 (1998).
5. J. J. Zayhowski, "Microchip lasers create light in small spaces," *Laser Focus World* **32**, 73 (1996).
6. J. J. Zayhowski, "Ultraviolet generation with passively *Q*-switched picosecond microchip lasers," *Opt. Lett.* **21**, 588 (1996); errata, 1618 (1996).
7. J. J. Zayhowski and C. Dill III, "Diode-pumped passively *Q*-switched picosecond microchip lasers," *Opt. Lett.* **19**, 1427 (1994).
8. S. Zhou, K. K. Lee, Y. C. Chen, and S. Li, "Monolithic self-*Q*-switched Cr,Nd:YAG laser," *Opt. Lett.* **18**, 511 (1993).
9. P. Wang, S.-H. Zhou, K. K. Lee, and Y. C. Chen, "Picosecond laser pulse generation in a monolithic self-*Q*-switched solid-state laser," *Opt. Commun.* **114**, 439 (1995).
10. L. Fulbert, J. Marty, B. Ferrand, and E. Molva, "Passively *Q*-switched monolithic microchip laser," *Conf. Lasers Electro-Optics Tech. Dig.* **15**, 176 (1995).
11. B. Braun, F. X. Kärtner, U. Keller, J.-P. Meyn, and G. Huber, "Passively *Q*-switched 180-ps Nd:$LaSc_3(BO_3)_4$ microchip laser," *Opt. Lett.* **21**, 405 (1996).
12. B. Braun, F. X. Kärtner, G. Zhang, M. Moser, and U. Keller, "56-ps passively *Q*-switched diode-pumped microchip laser," *Opt. Lett.* **22**, 381 (1997).
13. J. J. Degnan and J. F. McGarry, "SLR2000: eye-safe and autonomous single-photoelectron satellite laser ranging at kilohertz rates," SPIE **3218**, 63 (1997).